IEEE Access
Multidisciplinary | Rapid Review | Open Access Journal

Received September 27, 2020, accepted October 26, 2020, date of publication November 6, 2020,
date of current version November 19, 2020.

Digital Object Identifier 10.1109/ACCESS.2020.3036616

Optimal Resource Allocation and Interference Management for Multi-User Uplink Light Communication Systems With Angular Diversity Technology

HOSSIEN B. ELDEEB[1], (Member, IEEE), MONA HOSNEY[2], HANY M. ELSAYED[3], (Member, IEEE), RAGIA I. BADR[3], MURAT UYSAL[1], (Fellow, IEEE), AND HOSSAM A. I. SELMY[4], (Member, IEEE)

[1]Department of Electrical and Electronics Engineering, Özyeğin University, 34794 Istanbul, Turkey
[2]National Telecommunication Institute, Cairo 11432, Egypt
[3]Department of Electronics and Electrical Communications, Cairo University, Giza 12613, Egypt
[4]National Institute of Laser Enhanced Science (NILES), Cairo University, Giza 12613, Egypt

Corresponding author: Hossien B. Eldeeb (hossien.eldeeb@ozyegin.com)

The work of Hossien B. Eldeeb was supported by the European Horizon 2020 MSC ITN (VISION) under Grant 764461. The work of Mona Hosney was supported by the National Telecommunication Institute. The work of Murat Uysal was supported by the Turkish Scientific and Research Council (TUBITAK) under Grant 215E311.

ABSTRACT Light communication (LC) technology has been regarded as a promising candidate for future indoor wireless networks by providing safe, power-efficient, and high data rate communications needed for tomorrow's applications. Both visible light (VL) and infrared (IR) wavelengths can be utilized to design LC systems. It is often proposed that VL can be used to offload downlink traffic while near-IR is typically used in the uplink. In this paper, the uplink multi-user LC system is considered where the system performance is degraded by both inter-symbol interference (ISI) resulting from multipath reflections and inter-user interference (IUI) coming from neighboring users. To mitigate these limitations, an optimal fair resource allocation (OFRA) scheme is proposed which aims to improve the fairness among the users in terms of their received signal to interference plus noise ratios (SINRs) by implementing the angle diversity technology. Precisely, by assigning an ON/OFF state for each LED of the angle diversity transmitter (ADT), used by each user, the IUI can be significantly reduced. Also, the angle diversity receiver (ADR) is used to effectively mitigate the effects of ISI. The allocation matrix which achieves the highest fairness between different users is obtained for different scenarios of user distribution. Toward this, the exhaustive search (ES) method is used to obtain the optimal solution for the optimization problem under consideration. However, to reduce the time complexity of ES method, a quasi-optimal solution called sub-optimal fair resource allocation scheme SFRA is proposed. The sub-optimal solution is based on the genetic algorithm (GA) scheme. The simulation results reveal that both the OFRA and SFRA achieve almost the same performance. Moreover, the simulation results indicate the superior performance of the proposed OFRA scheme over the conventional single transmitter (ST) one.

INDEX TERMS Light communications, multi-user light communication networks, visible light communication, resource allocation, angular diversity, inter-user-interference, inter-symbol-interference.

I. INTRODUCTION

Nowadays, light communication (LC) technology is gaining more interest due to its huge available bandwidth in unregulated optical spectrum [1]. Both visible light (VL) and infrared (IR) wavelengths can be utilized to design LC systems which can be positioned as either alternative or complementary to radio communications [2], [3]. LC technology represents an attractive key which opens the doors for high data rate indoor wireless applications needed in daily life [2], [4]. It has the advantages of energy efficiency, inherent security, human health, and unregulated bandwidth [5], [6]. Nevertheless, there are several challenges limiting the realization and the marketability of the LC system in

The associate editor coordinating the review of this manuscript and approving it for publication was Jie Tang.

the fifth-generation (5G) wireless networks. One of these challenges is how to establish an efficient uplink LC channel, while achieving the envisioned Light-Fidelity (Li-Fi) communication systems [7]–[9]. Usually, in the downlink LC channel, visible light-emitting-diodes (LEDs) are used to achieve both illumination and data transmission. This is due to their unique advantages such as long lifetime, low cost, high data rate and lower power consumption compared to other artificial light sources [10]–[13].

However, using visible LEDs in the uplink channel leads to the excessive glare problem which has an intrusive impact on the human eye [14]. Additionally, the uplink light can interfere with the downlink reflected light, resulting in signal interference which limits the performance of LC system in high-speed transmission [15]. These issues drove the researchers towards complementing the downlink LC technology with another alternative uplink one. Therefore, some authors demonstrated the radio frequency (RF) waves and ultraviolet (UV) technologies to realize uplink channel [16], [17]. However, both RF and UV are harmful technologies and require complex implementation [18].

Generally, IR-LED has been regarded as one of the promising solutions avoiding the complexity and the interference with RF communication [18]. Also, it has the lowest effect on the human healthiness so it is widely used [13], [14], [19] and [20]. In [18], a surveillance camera based IR has been demonstrated for uplink connection which can overcome the glare and interference but it has a limitation on communication speed. An uplink LC system based on time division duplex (TDD) has been proposed in [21]. In [12], a 225 Mb/s uplink transmission can be realized by using sub-carrier multiplexing and wavelength division multiplexing (WDM). However, the WDM schemes are costly and complex. Additionally, the angle diversity technology has been used in the indoor LC systems and can significantly eliminate the effects of ambient noise and inter-symbol interference (ISI) resulting from multipath reflections [22]–[26].

Nevertheless, all the previously mentioned studies are confined to single user uplink transmission in the LC networks. Obviously, to make the LC systems practical for the envisioned Li-Fi system, multi-user (MU) uplink transmission has to be supported [27]–[29]. However, both inter-user interference (IUI) coming from neighboring users and ISI resulting from reflected signals could significantly degrade the performance of MU-LC networks. Therefore, efficient multiplexing and resource allocation schemes between different users are required to mitigate these interferences.

Recently, orthogonal code division multiple access (OCDMA) combined with TDD has been investigated as a promising multiple access (MA) scheme for indoor uplink LC system [7]. In that work, TDD is used for bidirectional data transmission and OCDMA is applied for MU access. The system has a limitation on the maximum number of active users due to the increasing length of spreading codes and effects of ISI and IUI. Orthogonal frequency division multiplexing with interleaving division multiple access scheme (OFDM-IDMA) has been proposed in [30] in order to solve these problems. However, these systems suffer high peak-to-average-power-ratio (PAPR) problem [31].

Non-orthogonal-multiple-access (NOMA) techniques offer a trade-off between fairness and throughput when used for LC systems [32]–[35]. In [34], the throughput of the downlink LC system with NOMA has been maximized while the user fairness has been maintained. In [35], the energy efficiency of bidirectional LC system with NOMA has been maximized by adopting a QoS-guaranteed optimal power allocation strategy. However, the users of NOMA systems suffer delay in services and imperfect interference reduction, especially in a high dense user network.

Recently, machine learning and deep learning algorithms have attracted much interest to solve the optimization problems encountered in MU-LC systems [36], [37]. In [36], the sum-rate maximization problem of LC with NOMA system has been investigated and then solved by utilizing the Harris hawks algorithm. In [37], the energy efficiency optimization problem of a dynamic unmanned aerial vehicles LC system has been addressed. In which, a machine learning algorithm based on gated recurrent units with convolutional neural networks has been proposed to minimize the transmit power while achieving the illumination and communication requirements of all users. In [38], a unified resource allocation scheme based on particle swarm optimization algorithm has been presented for indoor LC downlink channels. Also, an efficient LED assignment scheme has been proposed in [39] which can suppress the interference caused by simultaneous data transmission of LEDs and improve the overall SINR of the users. Nevertheless, these systems were focused only on the downlink channels. Therefore, the uplink MU transmission is still a major challenge for realizing LC networks. In [40], we have proposed the idea of using the angle diversity at both transmitter and receiver side in LC networks. To fairly distribute the resources between the users, the signal of the worst user has to be maximized by using an optimal fair resource allocation (OFRA) scheme.

The key contribution of this paper can be illustrated as the following:

- The uplink MU-LC system is realized by utilizing the IR wavelength avoiding sending light to base station, and by using the angle diversity technology at both transmitter and receiver side. Clearly, using the angle diversity receiver (ADR) can significantly reduce the inter-symbol interference (ISI) resulting from the multipath reflections. On the other side, utilizing the angle diversity transmitter ADT) for each user provides additional opportunities to enhance the system performance by reducing the inter-user interference (IUI).
- We propose an OFRA scheme which aims to enhance the fairness between all users in terms of their received signal to interference plus noise ratio (SINR) by switching on the most suitable LED of each ADT (user).
- The optimization problem under consideration is first formulated and the allocation matrix that achieves the

objective of such problem is obtained using two methods. As a benchmark, the exhaustive search (ES) method is used to obtain the optimal solution. On the other side, and to reduce the complexity, a sub-optimal solution is proposed by utilizing the genetic algorithm (GA) scheme and compared with the optimal solution.
- Different scenarios of user distributions are considered and the effect of transmitter viewing angle and receiver field of view (FOV) angle on the SINR is addressed at all scenarios under consideration.
- Since the most common underlining assumption in most works of uplink multi-user VLC systems [7], [30], [32], [41] is that the user has a single LED to establish its uplink communication link, the performance of proposed scheme is compared with the conventional single transmitter (ST) scheme in terms of the received SINR, average data rate, average number of blocked users, and fairness index.

The rest of this paper is organized as the following. The multi-user uplink LC system model with angle diversity technology is explained in section 2. Details of the proposed OFRA scheme are presented in section 3. Simulation results are discussed in section 4. Finally, the paper is concluded in section 5.

II. MULTI-USER UPLINK LC SYSTEM MODEL

Recently, in the downlink LC systems, ADR has been used to mitigate the effects of ambient noise and ISI from multipath reflections [22]–[25]. The basic idea of ADR is to use multiple photodetectors (PDs) that point in different directions with different normal unit vectors and incident angles, resulting in less correlated channel gain matrix between all LEDs and PDs. A further better variation of the conventional ADR is the constraint field of view ADR where the FOV angle of the ADR is optimized to also eliminate the line-of-sight (LOS) co-channel interference (CCI) in the downlink LC channel [42]. Furthermore, angle diversity transmitter (ADT) which contains multiple numbers of narrow beam IR-LEDs with different orientations, is used to improve the performance of LC systems [26], [40]. In this paper, the angle diversity technology is used at both transmitter and receiver sides in uplink LC channel to reduce both ISI and MU (CCI) interference as shown in Fig. 1. Clearly, this reduction is obtained by selecting and allocating the optimal transmitter and receiver pairs of all ADTs and ADRs.

The considered ADT design consists of L IR-LEDs. The first one is mounted on the top center of ADT structure and the other $(L-1)$ side LEDs are arranged uniformly in a circle of a certain radius along the plane of the top LED. Each LED has a different direction that can be defined by two angles; azimuth (γ^l_{LED}) and elevation (δ^l_{LED}) for $1 \leq l \leq L$. Therefore, the normal unit vector at l^{th} LED, $\hat{S}_l$ can be defined by its position and orientation angles as ($x^l_{LED}, y^l_{LED}, z^l_{LED}, \gamma^l_{LED}, \delta^l_{LED}$) as shown in Fig. 2. Similarly, the considered ADR consists of F PDs. These PDs are arranged to point in different directions which are verified by the azimuth and elevation

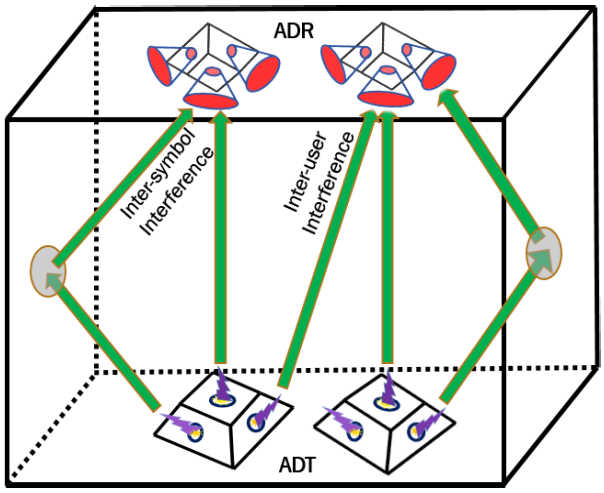

FIGURE 1. Multiuser uplink LC system using angle diversity technology.

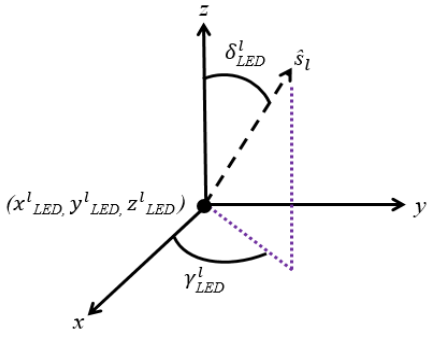

FIGURE 2. The orientation of l^{th} LED.

angles, γ^f_{PD} and δ^f_{PD}, respectively for $1 \leq f \leq F$. The first PD is placed horizontally on the top center of ADR structure and the other $(F-1)$ side PDs are arranged uniformly in a circle with a certain radius and with a fixed tilting angle along the plane of the top one. Thus, the normal unit vector of the f^{th} PD, $\hat{R}_f$ can be defined by its position and orientation angles as ($x^f_{PD}, y^f_{PD}, z^f_{PD}, \gamma^f_{PD}, \delta^f_{PD}$) which is similar to Fig. 2. Therefore, the uplink LC network with R ADRs has a total of $N = F \times R$ PDs. Clearly, in uplink MU-LC network, each PD receives a strong (main) signal from one user and interfering signals from the others, resulting in IUI problem that reduces the received SINRs. The goal of this paper is to optimally allocate the resources of the uplink channel to achieve the highest fairness among different users in terms of their received SINR.

Generally, in a LC system, the intensity modulation with direct detection (IM-DD) has been widely used [43]. The information data is carried with the intensity of propagated optical light. The uplink channel has both LOS and non-LOS (NLOS) propagation scenarios [22], [44]. The LOS channel model concerns with the signals that travel directly from the user (transmitter) to the PD receiver, while the NLOS channel model raises from reflected signals. The overall system channel gain is the sum of LOS and NLOS ones. Also, the noise at the PD receiver is modeled as additive white Gaussian

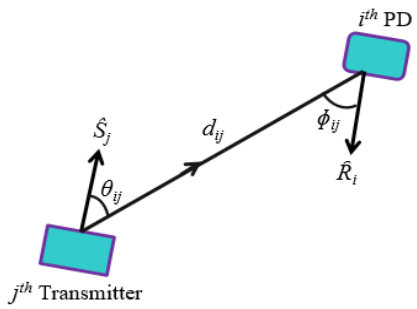

FIGURE 3. The LOS channel link between j^{th} transmitter and i^{th} PD.

noise (AWGN) [43], [44]. The uplink LC system with N PDs (receivers) and M users (active transmitters) can be modeled as a base band linear time-invariant one. The resultant output currents vector $y(t) = [y_1(t), y_2(t), \cdots, y_{N(t)}]$ of all PDs is given by [44], [45].

$$y(t) = \eta\, h(t) \otimes x(t) + n(t), \tag{1}$$

where $x(t) = [x_1(t), x_2(t), \cdots, x_M(t)]$ is the instantaneous transmitted optical power vector of all active transmitters, η is PD's responsivity, and $n(t) = [n_1(t), n_2(t), \cdots, n_N(t)]$ represents the AWGN vector at all PDs with zero mean and variance σ_n^2. The noise has two dominant components; thermal noise generated from receiver electronics with variance σ_{th}^2 and shot noise generated from received light with variance σ_{sh}^2, i.e, $\sigma_n^2 = \sigma_{th}^2 + \sigma_{sh}^2$ [44]. Also, $h(t)$ is the $N \times M$ channel impulse response matrix which summarizes the impulse responses between all transmitters and PDs as:

$$h(t) = \begin{pmatrix} h_{11}(t) & h_{12}(t) & \cdots & h_{1M}(t) \\ h_{21}(t) & h_{22}(t) & \cdots & h_{2M}(t) \\ \vdots & \ddots & \vdots & \\ h_{N1}(t) & h_{N2}(t) & \cdots & h_{NM}(t) \end{pmatrix}, \tag{2}$$

where $h_{ij}(t)$ is the channel impulse response between the j^{th} transmitter and the i^{th} PD. Clearly, this channel gain is the sum of LOS and NLOS channel gains, $h_{ij}^{los}(t)$ and $h_{ij}^{nlos}(t)$, respectively, as:

$$h_{ij}^{los}(t) = \begin{cases} \dfrac{(m_l+1)\, A \cos^{m_l}(\theta_{ij}) \cos(\phi_{ij})}{2\pi (d_{ij})^2} \\ \times \;\; G(\phi_{ij}) T(\phi_{ij}) \delta(t - \dfrac{d_{ij}}{c}), & \phi_{ij} \le \psi, \\ 0, & \phi_{ij} > \psi\,, \end{cases} \tag{3}$$

where A is the PD's area and m_l represents the Lambertian order of the LED transmitter which is related to half luminance semi angle Θ by $m_l = \frac{-\ln(2)}{\ln(\cos\Theta)}$. Also, θ_{ij}, ϕ_{ij} and d_{ij} are the angle of irradiance at LED transmitter j relative to PD i, the angle of incidence at PD i relative to LED transmitter j, and the distance between the LED transmitter j and the PD i, respectively as indicated in Fig. 3. Also, $T(\phi_{ij})$, $G(\phi_{ij})$ and c are the transmission coefficient of optical filter, the gain of optical concentrator, and the speed of light, respectively.

On the other side, to calculate the NLOS channel response, the room's walls are divided into K small reflecting elements.

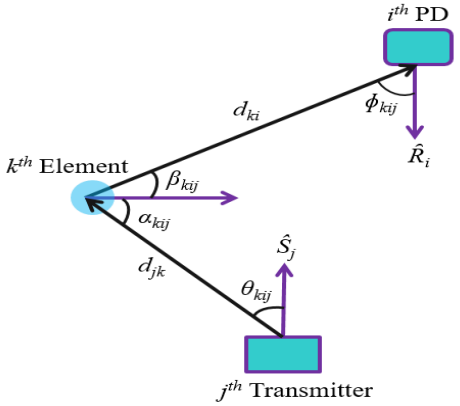

FIGURE 4. The NLOS channel link between j^{th} user and i^{th} PD reflected by the k^{th} element.

Each element k, where $k \in \{1, 2, \ldots, K\}$, has a small area dA and a reflection coefficient ρ. The element is treated as a small LED transmitter that emits light from its center in Lambertian pattern of an attenuated version of received signals [44]. In this paper, only the first order reflection is considered and the higher orders are neglected as they have much less power [20], [44]. The NLOS gain expression for a single reflection from all walls can be given by $h_{ij}^{nlos}(t) = \sum_{k=1}^{K} dh_{ijk}^{nlos}(t)$, where $dh_{ijk}^{nlos}(t)$ represents the NLOS channel response from LED transmitter j to PD i reflected by k^{th} wall element which is given as [43], [44]

$$dh_{ijk}^{nlos}(t) = \begin{cases} \dfrac{(m_l+1)\rho A \cos^{m_l}(\theta_{kij}) \cos(\alpha_{kij}) \cos(\beta_{kij}) \cos(\phi_{kij})}{2\pi^2 d_{jk}^2 d_{ki}^2} \\ \times\, G(\phi_{kij}) T(\phi_{kij}) dA_k \delta(t - \dfrac{d_{jk} + d_{ki}}{c}), & \phi_{kij} \le \psi, \\ 0, \quad \phi_{kij} > \psi, \end{cases} \tag{4}$$

where d_{jk} and d_{ki} are the distances from the LED transmitter j and the PD i to the center point of k^{th} reflecting element, respectively as shown in Fig. 4. And, θ_{kij} is the irradiance angle at the LED transmitter j with respect to reflecting element k. α_{kij} is the angle of incidence at the reflecting element k with respect to the LED transmitter j. Also, β_{kij} is the irradiance angle at the reflecting element k with respect to the PD i. Additionally, ϕ_{kij} is the incidence angle at the PD i relative to the reflecting element k as shown in Fig. 4. Finally, the total received optical power at i^{th} PD can be summarized by [44].

$$P_r^i(t) = \sum_{j=1}^{M} \{h_{ij}^{los}(t) + \sum_{k=1}^{K} dh_{ijk}^{nlos}(t)\} \otimes x_j(t). \tag{5}$$

III. FAIR RESOURCE ALLOCATION SCHEME

The considered uplink MU-LC network consists of M users and N PDs. Each user has an ADT with L IR-LEDs. However, to reduce the optimization dimensions and decrease amount of transmitted power of each ADT, only one of the ADTs'

LEDs is assumed to be on (active) at a time and the remaining $(L-1)$ LEDs are off. Moreover, the operating LEDs are assumed to transmit the same average optical power P_t, i.e. the transmitted power of LED l at user j, $P_{jl} = P_t$. The allocation (assignment) of operating LEDs for different users is made to reduce the IUI and enhance the performance of the overall network.

Generally, the on/off states of all LEDs associated with different users are summarized in the $(M \times L)$ allocation matrix A which can be given by

$$A = \begin{pmatrix} a_{11} & a_{12} & \cdots & a_{1L} \\ a_{21} & a_{22} & \cdots & a_{2L} \\ \vdots & \ddots & \vdots & \vdots \\ a_{M1} & a_{M2} & \cdots & a_{ML} \end{pmatrix}, \tag{6}$$

where a_{jl} is a binary allocation variable associated with l^{th} LED of user j. The value of this variable is equal to 1 when the LED is on and 0, otherwise. Also, as only one of the ADT's LEDs is on at a time, the sum of the allocation variables associated with each user is equal to one, i.e. $(\sum_{l=1}^{L} a_{jl} = 1), \forall\, j \in \{1, 2, \cdots, M\}$. Clearly, there exists many feasible allocation matrices that obey this constraint. Among these matrices, there is an optimal allocation matrix that achieves the highest fairness between all users by maximizing their minimum SINR.

Generally, at an allocation matrix A, we can define a vector $\bar{a} = [a_1^*, a_2^*, \ldots, a_M^*]$ which represents the active LED index of each user where, $a_j^* \in \{1, 2, \ldots, L\}$ is the index of active LED for j^{th} user at allocation vector $\bar{a}$ and $j \in \{1, 2, \cdots, M\}$. Also, the value of the binary variable a_{jl} can be given by

$$a_{jl} = \begin{cases} 1, & l = a_j^* \\ 0, & otherwise \end{cases} \tag{7}$$

The SINR between j^{th} user and i^{th} PD at $\bar{a}$, $\gamma_{ij}(\bar{a})$ including both IUI and ISI is calculated by

$$\gamma_{ij}(\bar{a}) = \frac{(\sum_{l=1}^{L} \eta P_t a_{jl} H_{ijl}^{los})^2}{\sigma_n^2 + \sum_{m=1, m\neq j}^{M} (\sum_{l=1}^{L} \eta P_t a_{ml} H_{iml}^{los})^2 + \sum_{m=1}^{M} (\sum_{l=1}^{L} \eta P_t a_{ml} H_{iml}^{nlos})^2} \tag{8}$$

where H_{iml}^{los} and H_{iml}^{nlos} are the LOS and NLOS DC channel gains for the link between the l^{th} LED of user j and the PD i, respectively. Clearly, at an allocation vector $\bar{a}$, PD i is assigned to the user that has highest SINR using assignment variable $U_i(\bar{a})$ as:

$$U_i(\bar{a}) = \arg \max_{j \in \{1,2,\cdots,M\}} \gamma_{ij}(\bar{a}), \quad \forall i \in \{1, 2, \cdots, N\}, \tag{9}$$

Therefore, the received SINR of user j at a given allocation vector $\bar{a}$, $\gamma_j(\bar{a})$ can be given by

$$\gamma_j(\bar{a}) = \begin{cases} \max_{i \in N} \gamma_{ij}(\bar{a}), & \forall\, i : j = U_i(\bar{a}) \\ 0, & \forall\, i : j \neq U_i(\bar{a}) \end{cases} \quad \forall j \in \{1, 2, \cdots, M\} \tag{10}$$

Clearly, Eq. (10) states that user j has a SINR value when it achieves the highest gain of at least one PD, otherwise its SINR is set to zero. In other words, when the user is not being received (hasn't the highest received power) with any PD, its SINR value is considered zero. Furthermore, when the user is assigned to more than one PD, its SINR value is the maximum one received by these PDs, i.e. the selection best combining (SBC) is implemented.

A. PROBLEM ASSUMPTIONS AND EXTENSIONS

Some assumptions are considered in the proposed work:

Firstly, all users are assumed to have the same number of LEDs in their ADTs (L LEDs). However, in case that some users have different numbers of LEDs with maximum number of L LEDs, the $(M \times L)$ allocation matrix A still can be formulated by setting the states of non existing LEDs to zero and the OFRA proceeds without changes.

Secondly, Since the main objective of this paper is to show the benefits of both angular diversity and the resource allocation strategy, we simplify the problem by assuming that the average transmitted power of all LEDs is constant as [26], [46], [47]. However, to enhance the system performance, adaptive power transmission with one of discrete levels could be implemented. Also, the fixed DC offset that is assumed in this work can be optimized to further enhance the performance of LC system. This will extend dimensions of the optimization problem under investigation and could be considered in the future research.

Thirdly, In the proposed uplink LC system, the number of served users should not exceed the number of the PDs in the ADRs. However, it is also possible to install additional/auxiliary ADR units which will be activated only when a large number of users is detected $(M > N)$. This will avoid the needles complexity in case of low number of users. Nowadays, the cost of detectors used in ADR units has been much reduced either for the p-i-n photodiodes [48] or for the CMOS avalanche ones [49]. Since the p-i-n photodiodes have the simplest and the lowest rugged structure, it has been widely used to construct the ADR units [22], [24], [25], [50].

B. OFRA FORMULATION

The objective of this optimization is to find the optimal allocation matrix $A^\star$ that maximizes the lowest SINR for all users under certain defined constraints. In other words, we aim to find the optimal vector $\bar{a}_{opt}$ which defines the index of active LEDs for all users in away to achieve the highest fairness among the users. Therefore, The max-min optimization is used to formulate this problem as [51]:

$$\max_{\bar{a}} \min_{j} \gamma_j(\bar{a}) \tag{11a}$$

$$s.t.\ a_{jl} = \begin{cases} 1, & l = a_j^* \\ 0, & otherwise \end{cases} \quad \forall j, l \tag{11b}$$

$$\sum_{l=1}^{L} a_{jl} = 1, \quad \forall j \tag{11c}$$

$$P_{jl} = P_t \quad \forall j, l \tag{11d}$$
$$j \in \{1, 2, \ldots, M\}, \quad l \in \{1, 2, \ldots, L\} \tag{11e}$$
$$i \in \{1, 2, \ldots, N\}, \quad a_j^* \in \{1, 2, \ldots, L\} \tag{11f}$$

In the above model, the first constraint (11b) indicates that the optimal LED of a user is switched on while the other LEDs are turned off at an allocation vector $\bar{a}$. The second constraint (11c) ensures that a user can be served by only one LED which achieves a fair comparison to the system with single transmitter for each user. The third constraint (11d) is imposed to guarantee that each LED of any user has the same average optical power, P_t.

The max-min problem in (11) can be transformed into an equivalent form by presenting an auxiliary parameter $\lambda = \min_j \gamma_j(\bar{a})$ which represents the worst-case SINR over all users. Clearly, when λ is maximized, it will be less than or equal to $\gamma_j(\bar{a})$, $\forall j \in M$. At the same time, the optimal value of λ will be no less than $\min_j \gamma_j(\bar{a})$ as λ has been maximized. Therefore, the optimal value of this parameter, λ^* will be as large as possible which will be exactly equal to $\min_j \gamma_j(\bar{a})$. Thus, we can rewrite the optimization problem of (11) as the following equivalent formulation:

$$\max_{\bar{a}} \ \lambda \tag{12a}$$
$$s.t. \ \gamma_j(\bar{a}) \geq \lambda \quad \forall j \tag{12b}$$
$$a_{jl} = \begin{cases} 1, & l = a_j^* \\ 0, & otherwise \end{cases} \quad \forall j, l \tag{12c}$$
$$\sum_{l=1}^{L} a_{jl} = 1, \quad \forall j \tag{12d}$$
$$P_{jl} = P_t \quad \forall j, l \tag{12e}$$
$$j \in \{1, 2, \ldots, M\}, \quad l \in \{1, 2, \ldots, L\} \tag{12f}$$
$$i \in \{1, 2, \ldots, N\}, \quad a_j^* \in \{1, 2, \ldots, L\} \tag{12g}$$

To obtain the optimal solution for the optimization problem in (12), the ES method is used. However, such method poses an unaffordable computational burden in real time implementation. Therefore, a quasi-optimal solution with lower cost, delay, and complexity can be utilized. Toward that, an algorithm called sub-optimal fair resource allocation (SFRA) scheme is proposed in the next subsection.

C. SUB-OPTIMAL SOLUTION

It is clear that the optimization problem in (12) still has a non-convex function since vector $\bar{a}$ has a nonlinear nature with discrete values. In order to have a convex optimization problem, however, the objective function as well as all feasible regions must be convex in their nature [52], [53]. Therefore, the optimization problem in (12) is discrete non-convex one with multi-objective optimizations.

Toward solve this problem, we utilize the GA scheme [54] which is well suited for solving such multi-objective problems [55]. This is due to that it treats simultaneously with a set of possible solutions called Population, and scan in different regions of the space [56]. This makes it a powerful method in getting a several set of solutions for difficult discrete and non-convex problems [57]. GA is considered one of the most popular heuristic algorithm schemes.The idea of these algorithms is to start with one feasible solution for the problem and try to progressively improve it. The detailed description of the proposed SFRA algorithm is indicated as Algorithm 1.

Algorithm 1 SFRA Algorithm

Inputs:
N, M, L, ϵ
Set the maximum iteration number k_{max}
Set iteration index $k = 0$
Generate random solution for $\bar{a}$
repeat
for $i = 1$ to N **do**
  for $j = 1$ to M **do**
    for $l = 1$ to L **do**
Construct (8) from the pilot signals
Compute $\lambda = \min_j \gamma_j(\bar{a})$
Update $\bar{a}$ with constraint $1 \leq a_j^* \leq L$
Solve problem (12) obtaining $\bar{a}_{opt}$ and λ_{opt}
$k \leftarrow k + 1$;
    end for
  end for
end for
until convergence to optimal solution or $k > k_{max}$

Generally, the calculation of SINRs for all users at given allocation matrix requires knowing of channel gains between each LED and PD in the network. Practically, these channel gains can be measured at ADRs side in real-time environment by transmitting known pilot patterns sequentially from each LEDs of all ADTs. Also, far ADTs can be allowed to transmit their pilot signals simultaneous in order to reduce system delay and overheads.

IV. SIMULATION RESULTS

The optimization problem of OFRA scheme is solved using GA scheme while the optimal solution is obtained using the ES method. Then, the performance of the proposed OFRA scheme is compared with ST scheme. The ST scheme is the transmitter that uses a single LED for each user which is a common underline assumption of most works in uplink multi-user VLC systems [7], [30], [32], [41]. We provide the comparison in terms of their received SINRs, number of blocked users, Jain's fairness, and achieved average data rates.

A. SIMULATION SETUP

The considered room dimensions are 5 m × 5 m × 3 m [44], [51]. The value of $\rho = 0.7$ is considered similar to [51], [58] while $dA = 1$ cm^2 is taken as [59]. Similar to [44], [58], [60], we assume only the first order reflection, $K = 1$ which is considered the highest power component of diffuse part. We assume a desktop with height of 1 m where the user devices are located [4], [22]. Four ADRs ($R = 4$) are used to

TABLE 1. Room and user simulation parameters.

Room Parameters	Values
Room dimensions	5 m × 5 m × 3 m
Wall reflection coefficient (ρ)	0.7
Number of reflections (K)	1
Reflective area of wall (dA)	1 cm^2
User Parameters (ADT)	**Values**
User height	1 m
User number (M)	5
LEDs number of each user (L)	(1), (5)
Azimuth of LEDs (γ_{LED})	(0°,90°,180°,270°,360°)
Elevation of LEDs (δ_{LED})	(180°,45°,45°,45°,45°)
Power of each LED transmitter (P_t)	1 w
Radius of user distributions (r_u)	1 m

TABLE 2. Receiver simulation parameters.

Receiver Parameters (ADR)	Values
ADR number (R)	4
Locations of ADRs	(1.25,1.25), (3.75,1.25), (3.75,3.75),(1.25,3.75)
PDs number of each ADR (F)	5
Azimuth of PDs (γ_{PD})	(0°,90°,180°,270°,360°)
Elevation of PDs (δ_{PD})	(180°,45°,45°,45°,45°)
Responsivity of PD (R)	0.53 A/W
Optical filter gain $T_f(\phi)$	1
Concentrator refractive index $g_c(\phi)$	1.47
Area of PD (A_{PD})	1 cm^2
Absolute temperature (T_k)	300 K
Open-loop voltage gain (G_{olv})	10
PD Fixed capacitance (F_{cap})	112 pF/cm^2
FET channel noise factor (F_{fact})	1.5
FET trans-conductance (g_m)	30 mS
Boltzmann's constant(k)	1.3806488×10^{-23}
Noise-bandwidth factor (I_2)	0.562
Noise bandwidth factor (I_3)	0.0868
background current (I_b)	5100 μA
Bandwidth (B)	25 MHz

receive data signals from all users. The ADRs are installed at the room ceiling ($z = 3$ m) and face downwards. Each ADR has five PDs ($F = 5$) pointed in different directions. Also, five users ($M = 5$) are considered in the evaluations. Each user has an ADT that faces upwards and consists of five LED transmitters ($L = 5$) pointed in different directions. All LEDs transmit same average optical power of $P_t = 1\ W$ [22]. The LED bandwidth is assumed as $B = 25$ MHz [1, Table 7.1]. Additional simulation parameters are indicated in Tables. 1 and 2 which are taken similar to [42], [44], [51], [61].

It can be noted that the number of LEDs/PDs in the ADT/ADR of the considered LC system, same as the elevations of LEDs/PDs are assumed to be fixed to reduce the dimensions of the optimization problem. However, to further enhance the system performance, these parameters can be also optimized which has been already reported in [25], [62]. It has been verified in [25] that the SINR fluctuation could be gradually reduced when the number of LEDs/PDs increases. Therefore, our selection of 5 LEDs/PDs is in a good agreement with [25]. It has been also shown that both the large and the small elevation angles raise the SINR fluctuations particularly when many transmitters are used. Therefore, we consider the middle value of 45° for the elevation of LEDs/PDS of the ADT/ADR under investigation.

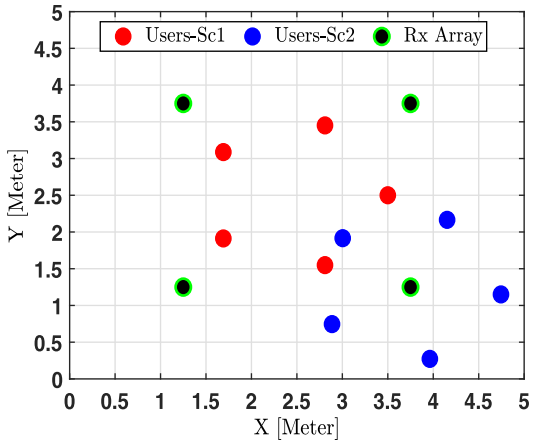

FIGURE 5. The user distribution inside the room for two scenarios. Red circles indicate the user's locations for first scenario and blue circles indicates the user's locations for second one. While, green circles show the ADR positions where $R = 4$ and $M = 5$.

Two scenarios of user distributions are considered in the carried evaluations. The first distribution scenario is the normal one in which the users are arranged symmetrically in a circle at room's center (2.5, 2.5, 1) with radius r_u =1 m as shown in Fig. 5 (red circles). The second scenario represents the worst one, where center of the circle is moved to the corner area of the room at position (3.75, 1.25, 1) as shown in Fig. 5 (blue circles).

B. SIGNAL TO INTERFERENCE PLUS NOISE RATIO (SINR) ANALYSIS

In order to evaluate the SINR for certain user at given allocation matrix, its corresponding PDs are first determined where it achieves the highest channel gains. Then, its SINR is selected to be the highest one received by these PDs (SC diversity). However, if the user has no corresponding PDs, its SINR value is set to zero. Clearly, the proposed OFRA scheme aims to maximize the minimum SINR value in the network.

Figure 6 indicates the convergence of SFRA scheme. Clearly, at most scenarios the algorithm converges before performing 600 iterations which enables its real time implementation. The performance comparison between ES and SFRA algorithms is presented in Fig. 7 after performing 700 iterations. The comparison is carried for two scenarios of users' distributions with PDs' FOV and LEDs' semi-angles of 45°. For the minimum SINRs which associated with user 3, the two schemes show nearly the same values which equal to 12.7 dB and 13 dB using GA and ES, respectively. However, for the rest users, there are slight differences in the performance of the two schemes. In scenario 1, ES scheme achieves an increasing of 2.5 dB in the SINR of user 5 while it achieves a decreasing of the same amount for user 2. Clearly, increasing the number of the performed iterations in SFRA algorithm would reduce the performance variation between the two schemes. However, the average SINR values of the two schemes show nearly same values. For example, consider Sc 1, the calculated average SINRs of all users are 17.3 dB and 17.55 dB using GA and ES scheme, respectively.

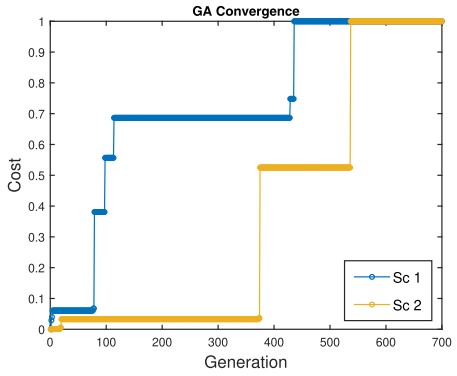

FIGURE 6. Cost of solution obtained by SFRA scheme at each generation for Scenario 1 and scenario 2. $\Theta = \psi = 45°$.

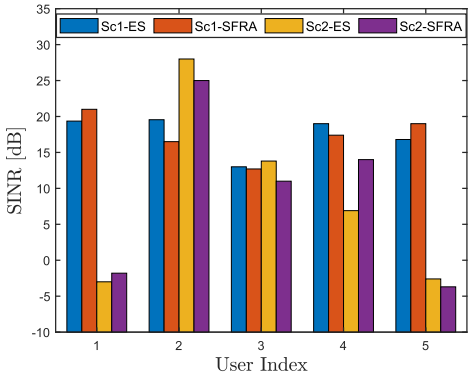

FIGURE 7. The SINR value of each user for SFRA and ES schemes. $\Theta = \psi = 45°$.

It is obvious that a small gap < 0.5 dB is existing between the proposed SFRA and the ES (Optimal solution) methods. On contrast, a significant reduction in the complexity can be achieved. The complexity of ES is given by $\mathcal{O}(M^L)$. For example, consider Sc1 and Sc2 where $M = L = 5$. The required iteration number of ES method is 3125 iterations. This can be much reduced using SFRA method to 438 and 537 iterations for Sc1 and Sc2, respectively.

The SINR performance of OFRA scheme is compared to that is achieved by ST one. In Fig. 8, the minimum and the average SINR of OFRA and ST users are plotted versus the PD's FOV angle ψ at LED semi-angle, $\Theta = 45°$. Obviously, OFRA scheme gives higher average and minimum SINR values than ST at all FOV values in the two scenarios. Approximately, improvements of 25 dB and 20 dB in average SINR along with enhancement of 50 dB and 30 dB in minimum SINR are achieved in Sc1 and Sc2, respectively. Furthermore, in OFRA scheme a small SINR gap exists between minimum and average SINR values resulting in higher fairness than that is achieved by ST scheme.

Fig. 9 indicates minimum and average SINR performance at LED's semi-angle of $\Theta = 60°$. Still, OFRA scheme outperforms the ST one in terms of minimum and average SINRs. However, increasing LED's semi-angle decreases performance gap between OFRA and ST schemes as ADTs become acting like STs.

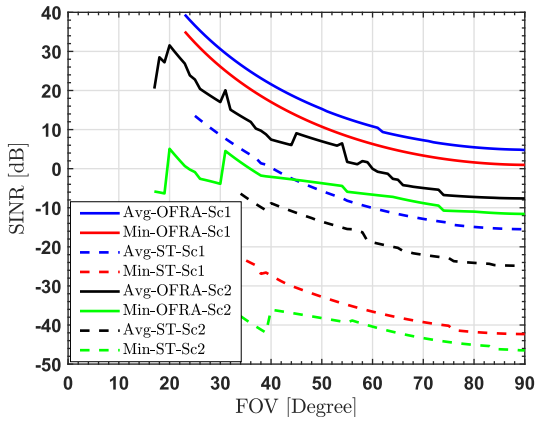

FIGURE 8. The average and the minimum SINR performance versus FOV angle of the PD for FRA and ST schemes. The semi-angle of the LED $\Theta = 45°$.

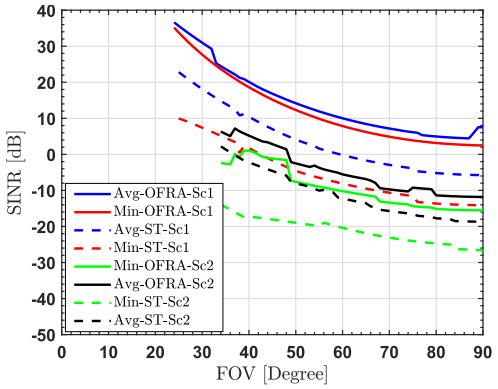

FIGURE 9. The average and the minimum SINR performance versus FOV angle of the PD for OFRA and ST schemes. The semi-angle of the LED $\Theta = 60°$.

Figs. 10 and 11 indicate the SINR performance versus the LED's semi-angle. In Fig. 10, average and minimum SINRs for the two scenarios are shown at PD's FOV angle of $\psi = 45°$. Clearly, OFRA scheme achieves higher minimum and average SINRs than that of ST scheme. However, The highest performance gap is obtained at LED's semi-angle near 40° and the gap decreases significantly by increasing semi-angle value. Fig. 11 indicates the minimum and average SINRs performance at PD's FOV angle of $\psi = 60°$. Clearly, increasing PD's FOV angle will increase IUI levels resulting in lower SINR.

The fairness of the two schemes is compared in terms of received SINR for all users at different values of PD's FOV angle and LED's semi-angle as indicated in Figs. 12 to 15. Fig. 12 indicates the users' SINR at PD's FOV angle $\psi = 45°$ and LED's semi-angle $\Theta = 45°$. Clearly, OFRA scheme achieves higher fairness levels than that of ST one. Furthermore, using ST scheme, second and fifth users in the first scenario and third and fourth users in the second scenario are blocked due to the increased levels of IUIs. Also, as indicated in Figs. 12 to 15, increasing the values of PD's FOV angle and/or LED's semi-half angle will decrease the received SINR for all users in OFRA scheme. In contrast,

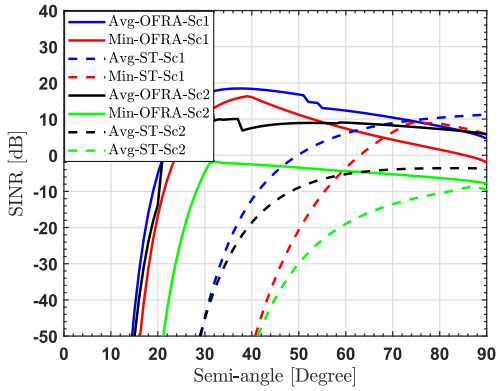

FIGURE 10. The average and the minimum SINR performance versus the semi-angle of the LED for OFRA and ST schemes. The FOV angle of the PD $\psi = 45°$.

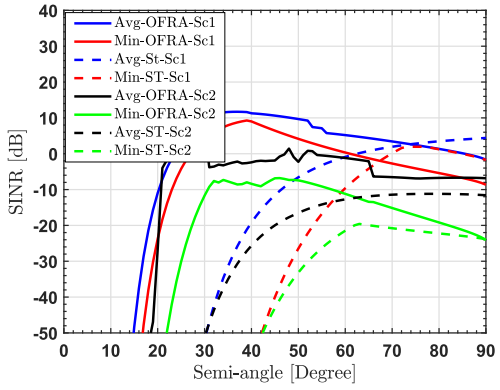

FIGURE 11. The average and the minimum SINR performance versus the semi-angle of the LED for OFRA and ST schemes. The FOV angle of the PD $\psi = 60°$.

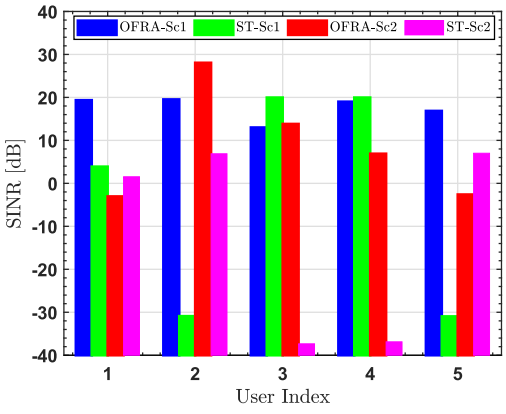

FIGURE 12. The SINR performance of each user with OFRA and ST schemes at the two scenarios. $\psi = \Theta = 45°$.

the performance of ST scheme is improved by increasing the values of these angles.

C. EFFECT OF NUMBER OF USERS

In this section the effect of number of users on the performance of OFRA scheme is evaluated. Toward that, given number of active users in the system, many scenarios for users distributions are randomly generated and average values of the performance metrics are computed over these scenarios.

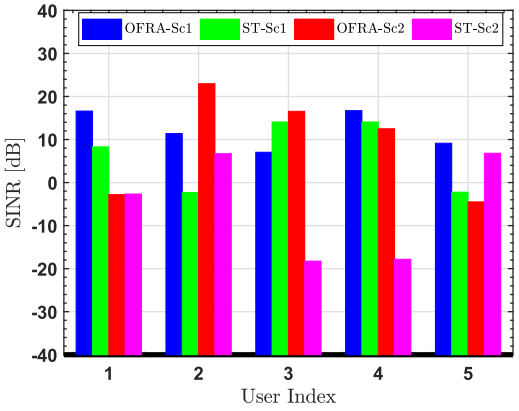

FIGURE 13. The SINR performance of each user with OFRA and ST schemes at the two scenarios. $\psi = 60°$, $\Theta = 45°$.

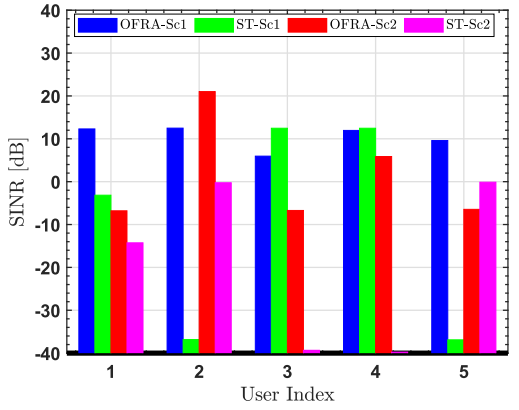

FIGURE 14. The SINR performance of each user with OFRA and ST schemes at the two scenarios. $\psi = 45°$, $\Theta = 60°$.

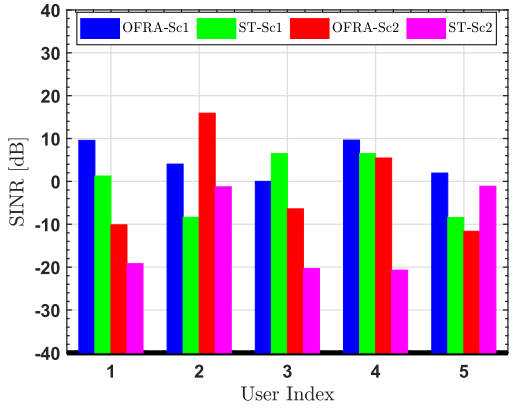

FIGURE 15. The SINR performance of each user with OFRA and ST schemes at the two scenarios. $\psi = 60°$, $\Theta = 60°$.

Fig. 16 indicates the effect of increasing number of users on both minimum and average SINR for OFRA and ST schemes. Clearly, at small and moderate numbers of active users less than 7 users, the OFRA schemes has a noticeable performance improvement over ST one. However, at large number of active users, the OFRA's performances approaches that of ST scheme.

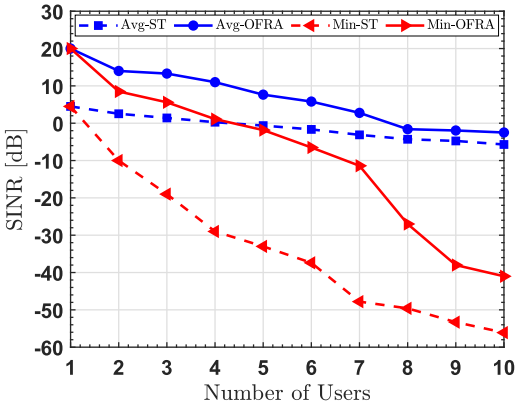

FIGURE 16. The average and the minimum SINR of OFRA and ST schemes versus number of users at $\psi = \Theta = 45°$.

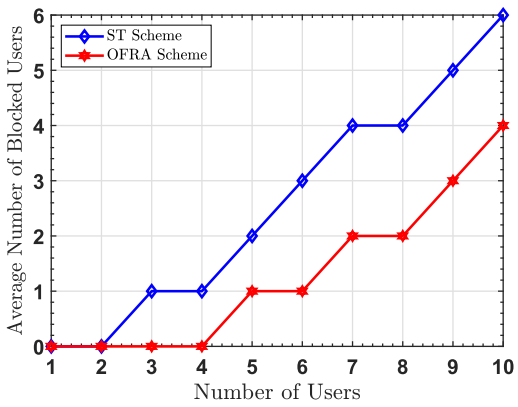

FIGURE 17. The average number of blocked users versus number of users at $\psi = 45°$, $\Theta = 45°$.

In Fig. 17, the average number of blocked users are indicated for OFRA and ST schemes. The OFRA can prevent blocking for four users while ST can do that for only two users. Also, at any number of users, the OFRA results in smaller number of blocked users compared to ST scheme.

D. FAIRNESS AND ACHIEVABLE DATA RATE

Generally, increasing number of supported users results in high levels of IUI which in turn decreases SINR and data rates of the users. The capacity of j^{th} user can be calculated by [63]:

$$C_j = B \log_2(1 + \gamma(j)) \tag{13}$$

where B is the communication system bandwidth. Fig. 18 indicates the average user's data rate versus the number of users for both OFRA and ST schemes. For number of users less than 7, the OFRA scheme achieves higher average data rate than that of ST scheme. Although, for number of users higher than 7, the ST achieves near the average data rate of OFRA scheme but at much less fairness among the users.

One of the main objectives of the OFRA scheme is to enhance the fairness between different users in terms of their data rates. In the evaluation of fairness performance, Jain's

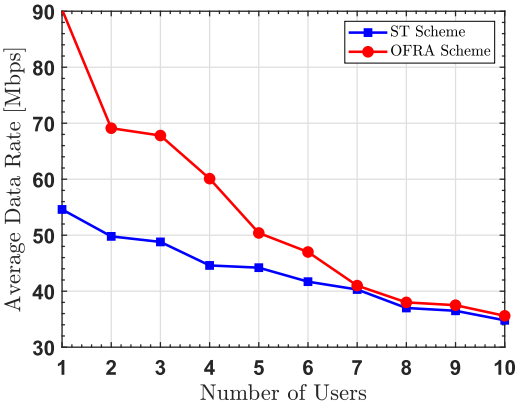

FIGURE 18. The average data rate versus number of users for OFRA and ST schemes at $\psi = \Theta = 60°$.

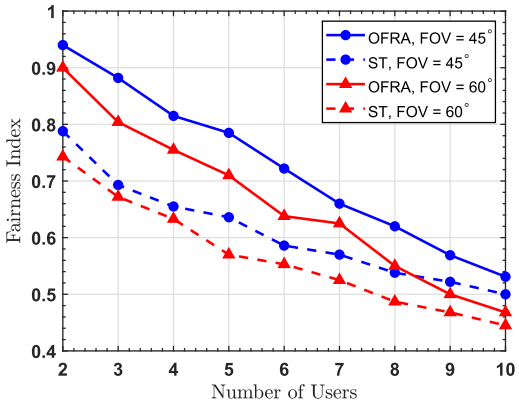

FIGURE 19. The fairness of OFRA and ST schemes versus number of users at $\Theta = 45°$.

fairness index (JFI) is used as [63]:

$$JFI = \frac{(\sum_{j=1}^{M} C_j)^2}{M \sum_{j=1}^{M} C_j^2} \tag{14}$$

Fig. 19 shows the Jain's fairness achieved for OFRA and ST schemes versus number of users at LED's semi-angle of 45°. The fairness is plotted for two PD's FOV angles which are 45° and 60°. The OFRA scheme has noticeable higher bit-rate fairness than ST scheme at any number of users. Furthermore, the fairness is increased in both OFRA and ST schemes by decreasing the PD'S FOV angle. This is due to the reduction in received IUI and ISI values. Numerically, at five users, OFRA scheme achieves a fairness index of 0.78 and 0.71 at $\psi = 45°$ and 60°, respectively. Also, the fairness gap between OFRA and ST scheme is much decreased at larger number of users. In Fig. 20, the same system is evaluated when the semi-angle is raised to 60°. However, increasing the semi-angle decreases fairness among the users in OFRA and ST schemes.

Thus, it is clear that OFRA scheme achieves the higher fairness at all cases than that of ST scheme. The reason for this is that the conventional ST scheme utilizes a single LED for each user which is only used to establish the communication link regardless to the position of the user and the corresponding received SINR value. At some places, however, the user

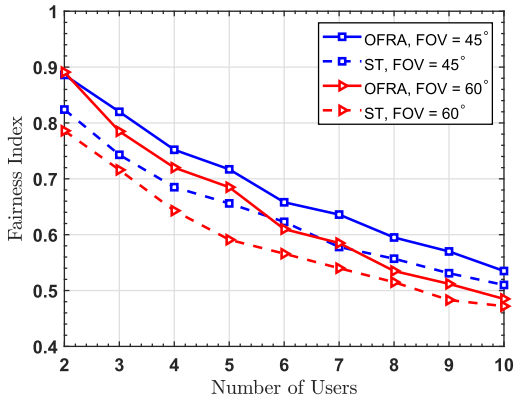

FIGURE 20. The fairness of OFRA and ST schemes versus number of users at $\Theta = 60°$.

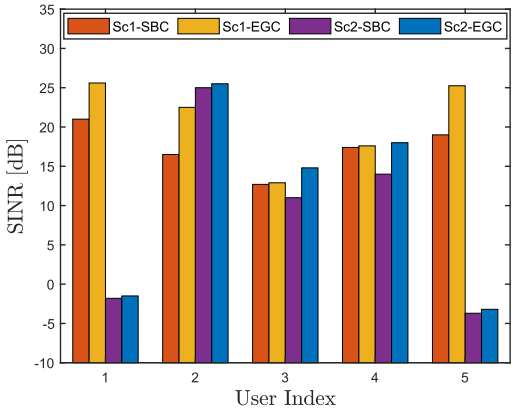

FIGURE 21. The SINR value of each user for SBC and EGC schemes. $\Theta = \psi = 45°$.

might be not able to establish a robust communication link using such single LED. Also, at other places, many users will communicate using their single LEDs to the same PD at the receiver side which will result in severe interference impact. As a result, the performance of the uplink LC system will be much affected, and some users might lose their connections such as user 3 and 4 in Sc2 (See Figs. 12 and 14). Further increasing in the number of users increases the average number of blocked users as mention before and depicted in Fig. 17. Therefore, by using the conventional ST scheme, the achievable data rate same as the fairness between the users are inferior comparing with the proposed OFRA scheme (See Figs. 18-20).

E. EQUAL GAIN COMBINING

So far, we assumed the deployment of SBC scheme where each user communicates with only one PD that can achieve the highest SINR value. It is possible to take advantage of the rest PDs. For this purpose, we utilize equal gain combining (EGC) scheme. EGC uses a direct sum of the branch signals from all rest PDs with equal weighting to all branches, which result in increasing of overall received SINR. The performance comparison between the two schemes is depicted in Fig. 21. The comparison is carried for both Sc1 and Sc2 of users' distributions with PDs' FOV and LEDs' semi-angles of 45°. As observed from Fig. 21, the achievable SINR of all users increases for all scenarios under consideration. One can notice a significant improvement (6 dB) for some users while for other users, a slight improvement (0.25 dB) can be only achieved. Clearly, this is based on the orientation of the user, the number of suitable PDs, and the number of interfering users at the position of such user.

V. CONCLUSION

In this paper, a new resource allocation scheme named OFRA has been proposed in the uplink multi-user LC network. The proposed OFRA scheme deploys the angle diversity technology at both transmitter and receiver sides to improve the fairness and reliability of the uplink channel. A GA scheme has been utilized to obtain the allocation matrix that achieves the highest fairness between the users. The results of GA have been compared with the ES method which obtains the optimal solution. The performance of the OFRA scheme has been compared to the conventional ST one. The simulation results reveal that the proposed OFRA scheme outperforms the conventional ST one in terms of received SINR, number of blocked users, Jain's fairness, and achieved average data rate at all users scenarios under consideration.

REFERENCES

[1] S. Dimitrov and H. Haas, *Principles of LED Light Communications: Towards Networked Li-Fi*. Cambridge, U.K.: Cambridge Univ. Press, 2015.
[2] Y.-D. Lin, "Editorial: Third quarter 2018 IEEE communications surveys and tutorials," *IEEE Commun. Surveys Tuts.*, vol. 20, no. 3, pp. 1607–1615, 3rd Quart., 2018.
[3] H. Abuella, M. Elamassie, M. Uysal, Z. Xu, E. Serpedin, K. A. Qaraqe, and S. Ekin, "Hybrid RF/VLC systems: A comprehensive survey on network topologies, performance analyses, applications, and future directions," 2020, *arXiv:2007.02466*. [Online]. Available: http://arxiv.org/abs/2007.02466
[4] A. T. Hussein, M. T. Alresheedi, and J. M. H. Elmirghani, "20 Gb/s mobile indoor visible light communication system employing beam steering and computer generated holograms," *J. Lightw. Technol.*, vol. 33, no. 24, pp. 5242–5260, Dec. 15, 2015.
[5] Y. Zhuang, L. Hua, L. Qi, J. Yang, P. Cao, Y. Cao, Y. Wu, J. Thompson, and H. Haas, "A survey of positioning systems using visible LED lights," *IEEE Commun. Surveys Tuts.*, vol. 20, no. 3, pp. 1963–1988, 3rd Quart., 2018.
[6] J. Luo, L. Fan, and H. Li, "Indoor positioning systems based on visible light communication: State of the art," *IEEE Commun. Surveys Tuts.*, vol. 19, no. 4, pp. 2871–2893, 4th Quart., 2017.
[7] S. V. Tiwari, A. Sewaiwar, and Y.-H. Chung, "Uplink bidirectional efficient multiuser visible light communications using TDD and diversity techniques," in *Proc. 8th Int. Conf. Ubiquitous Future Netw. (ICUFN)*, Jul. 2016, pp. 225–230.
[8] J. Chen, C. Yu, Z. Wang, J. Shen, and Y. Li, "Indoor optical wireless integrated with white LED lighting: Perspective & challenge," in *Proc. 10th Int. Conf. Opt. Commun. Netw. (ICOCN)*, Dec. 2011, pp. 1–2.
[9] D. Tsonev, S. Videv, and H. Haas, "Light fidelity (Li-Fi): Towards all-optical networking," *Proc. SPIE*, vol. 9007, Feb. 2014, Art. no. 900702.
[10] Z. Ghassemlooy, S. Arnon, M. Uysal, Z. Xu, and J. Cheng, "Emerging optical wireless communications-advances and challenges," *IEEE J. Sel. Areas Commun.*, vol. 33, no. 9, pp. 1738–1749, Sep. 2015.
[11] G. Cossu, A. M. Khalid, P. Choudhury, R. Corsini, and E. Ciaramella, "34 Gbit/s visible optical wireless transmission based on RGB LED," *Opt. Express*, vol. 20, no. 26, p. B501, 2012.
[12] Y. Wang, Y. Wang, N. Chi, J. Yu, and H. Shang, "Demonstration of 575-Mb/s downlink and 225-Mb/s uplink bi-directional SCM-WDM visible light communication using RGB LED and phosphor-based LED," *Opt. Express*, vol. 21, no. 1, pp. 1203–1208, 2013.
[13] Y. Wang, J. Yu, and N. Chi, "Symmetrical full-duplex integrated passive optical network and optical wireless communication transmission system," *J. Opt. Commun. Netw.*, vol. 7, no. 7, pp. 628–633, 2015.

[14] M. T. Alresheedi, A. T. Hussein, and J. M. H. Elmirghani, "Uplink design in VLC systems with IR sources and beam steering," *IET Commun.*, vol. 11, no. 3, pp. 311–317, Feb. 2017.

[15] P. Perez-Nicoli, F. Silveira, X. Zhang, and A. Amara, "Uplink wireless transmission overview in bi-directional VLC systems," in *Proc. IEEE Int. Conf. Electron., Circuits Syst. (ICECS)*, Dec. 2016, pp. 588–591.

[16] M. B. Rahaim, A. M. Vegni, and T. D. C. Little, "A hybrid radio frequency and broadcast visible light communication system," in *Proc. IEEE GLOBECOM Workshops (GC Wkshps)*, Dec. 2011, pp. 792–796.

[17] Z. Xu and B. M. Sadler, "Ultraviolet communications: Potential and state-of-the-art," *IEEE Commun. Mag.*, vol. 46, no. 5, pp. 67–73, May 2008.

[18] T.-C. Bui and S. Kiravittaya, "Demonstration of using camera communication based infrared LED for uplink in indoor visible light communication," in *Proc. IEEE 6th Int. Conf. Commun. Electron. (ICCE)*, Jul. 2016, pp. 71–76.

[19] H. B. Eldeeb, M. Uysal, S. Mana, P. Hellwig, J. Hilt, and V. Jungnickel, "Channel modelling for light communications: Validation of ray tracing by measurements," in *Proc. 12th IEEE IET Int. Symp. Commun. Syst., Netw. Digit. Sign. (CSNDSP)*, Jul. 2020, pp. 1–7.

[20] D. O'Brien, R. Turnbull, H. Le Minh, G. Faulkner, O. Bouchet, P. Porcon, M. El Tabach, E. Gueutier, M. Wolf, L. Grobe, and J. Li, "High-speed optical wireless demonstrators: Conclusions and future directions," *J. Lightw. Technol.*, vol. 30, no. 13, pp. 2181–2187, Jul. 2012.

[21] Y. F. Liu, C. H. Yeh, C. W. Chow, Y. Liu, Y. L. Liu, and H. K. Tsang, "Demonstration of bi-directional LED visible light communication using TDD traffic with mitigation of reflection interference," *Opt. Express*, vol. 20, no. 21, pp. 23019–23024, Oct. 2012.

[22] M. T. Alresheedi and J. M. Elmirghani, "Hologram selection in realistic indoor optical wireless systems with angle diversity receivers," *J. Opt. Commun. Netw.*, vol. 7, no. 8, pp. 797–813, 2015.

[23] Z. Zeng, M. D. Soltani, M. Safari, and H. Haas, "Angle diversity receiver in LiFi cellular networks," in *Proc. IEEE Int. Conf. Commun. (ICC)*, May 2019, pp. 1–6.

[24] H. B. Eldeeb, H. A. I. Selmy, H. M. Elsayed, and R. I. Badr, "Co-channel interference cancellation using constraint field of view ADR in VLC channel," in *Proc. IEEE Photon. Conf. (IPC) Part II*, Oct. 2017, pp. 1–2.

[25] C. Chen, W.-D. Zhong, H. Yang, S. Zhang, and P. Du, "Reduction of SINR fluctuation in indoor multi-cell VLC systems using optimized angle diversity receiver," *J. Lightw. Technol.*, vol. 36, no. 17, pp. 3603–3610, Sep. 1, 2018.

[26] Z. Chen, D. A. Basnayaka, and H. Haas, "Space division multiple access for optical attocell network using angle diversity transmitters," *J. Lightw. Technol.*, vol. 35, no. 11, pp. 2118–2131, Jun. 1, 2017.

[27] S. Al-Ahmadi, O. Maraqa, M. Uysal, and S. M. Sait, "Multi-user visible light communications: State-of-the-art and future directions," *IEEE Access*, vol. 6, pp. 70555–70571, 2018.

[28] Q. Wang, Z. Wang, and L. Dai, "Multiuser MIMO-OFDM for visible light communications," *IEEE Photon. J.*, vol. 7, no. 6, pp. 1–11, Dec. 2015.

[29] B. Li, J. Wang, R. Zhang, H. Shen, C. Zhao, and L. Hanzo, "Multiuser MISO transceiver design for indoor downlink visible light communication under per-LED optical power constraints," *IEEE Photon. J.*, vol. 7, no. 4, pp. 1–15, Aug. 2015.

[30] A. Kuriharat, C.-J. Ahn, T. Omori, and K.-Y. Hashimoto, "An application of OFDM-IDMA to uplink multiuser visible light communication system," in *Proc. Int. Symp. Intell. Signal Process. Commun. Syst. (ISPACS)*, Nov. 2015, pp. 412–416.

[31] H. B. Eldeeb, H. A. I. Selmy, H. M. Elsayed, F. E. Abd El-Samie, and R. I. Badr, "Visible light communication based on CPM-OFDM with chaotic interleaving scheme," in *Proc. IEEE Photon. Conf. (IPC)*, Oct. 2017, pp. 241–242.

[32] X. Guan, Q. Yang, and C.-K. Chan, "Joint detection of visible light communication signals under non-orthogonal multiple access," *IEEE Photon. Technol. Lett.*, vol. 29, no. 4, pp. 377–380, Feb. 15, 2017.

[33] H. Liu, P. Zhu, Y. Chen, and M. Huang, "Power allocation for downlink hybrid power line and visible light communication system," *IEEE Access*, vol. 8, pp. 24145–24152, 2020.

[34] Z. Yang, W. Xu, and Y. Li, "Fair non-orthogonal multiple access for visible light communication downlinks," *IEEE Wireless Commun. Lett.*, vol. 6, no. 1, pp. 66–69, Feb. 2017.

[35] C. Chen, S. Fu, X. Jian, M. Liu, X. Deng, and Z. Ding, "NOMA for energy-efficient LiFi-enabled bidirectional IoT communication," 2020, *arXiv:2005.10104*. [Online]. Available: http://arxiv.org/abs/2005.10104

[36] Q.-V. Pham, T. Huynh-The, M. Alazab, J. Zhao, and W.-J. Hwang, "Sum-rate maximization for UAV-assisted visible light communications using NOMA: Swarm intelligence meets machine learning," *IEEE Internet Things J.*, vol. 7, no. 10, pp. 10375–10387, Oct. 2020.

[37] Y. Wang, M. Chen, Z. Yang, T. Luo, and W. Saad, "Deep learning for optimal deployment of UAVs with visible light communications," 2019, *arXiv:1912.00752*. [Online]. Available: http://arxiv.org/abs/1912.00752

[38] M. S. Demir, S. M. Sait, and M. Uysal, "Unified resource allocation and mobility management technique using particle swarm optimization for VLC networks," *IEEE Photon. J.*, vol. 10, no. 6, pp. 1–9, Dec. 2018.

[39] Y. S. Eroglu, I. Guvenc, A. Sahin, Y. Yapici, N. Pala, and M. Yuksel, "Multi-element VLC networks: LED assignment, power control, and optimum combining," *IEEE J. Sel. Areas Commun.*, vol. 36, no. 1, pp. 121–135, Jan. 2018.

[40] H. B. Eldeeb, H. A. I. Selmy, H. M. Elsayed, R. I. Badr, and M. Uysal, "Efficient resource allocation scheme for multi-user hybrid VLC/IR networks," in *Proc. IEEE Photon. Conf. (IPC)*, Sep. 2019, pp. 1–2.

[41] X. Guan, Y. Hong, Q. Yang, and C. C.-K. Chan, "Non-orthogonal multiple access with phase pre-distortion in visible light communication," *Opt. Express*, vol. 24, no. 22, pp. 25816–25823, Oct. 2016.

[42] H. B. Eldeeb, H. A. I. Selmy, H. M. Elsayed, and R. I. Badr, "Interference mitigation and capacity enhancement using constraint field of view ADR in downlink VLC channel," *IET Commun.*, vol. 12, no. 16, pp. 1968–1978, Oct. 2018.

[43] J. M. Kahn and J. R. Barry, "Wireless infrared communications," *Proc. IEEE*, vol. 85, no. 2, pp. 265–298, Feb. 1997.

[44] T. Komine and M. Nakagawa, "Fundamental analysis for visible-light communication system using LED lights," *IEEE Trans. Consum. Electron.*, vol. 50, no. 1, pp. 100–107, Feb. 2004.

[45] H. Elgala, R. Mesleh, and H. Haas, "An LED model for intensity-modulated optical communication systems," *IEEE Photon. Technol. Lett.*, vol. 22, no. 11, pp. 835–837, Jun. 2010.

[46] S. Shao, A. Khreishah, M. Ayyash, M. B. Rahaim, H. Elgala, V. Jungnickel, D. Schulz, T. D. Little, J. Hilt, and R. Freund, "Design and analysis of a visible-light-communication enhanced WiFi system," *IEEE/OSA JOCN*, vol. 7, no. 10, pp. 960–973, Oct. 2015.

[47] S. V. Tiwari, A. Sewaiwar, and Y.-H. Chung, "Smart home multi-device bidirectional visible light communication," *Photonic Netw. Commun.*, vol. 33, no. 1, pp. 52–59, Feb. 2017.

[48] A. Bishnu, S. K. Das, M. Soni, and V. Bhatia, "Comparative analysis of low cost photodetectors for visible light communication," in *Proc. IEEE Int. Conf. Adv. Netw. Telecommun. Syst. (ANTS)*, Dec. 2018, pp. 1–6.

[49] B. Fahs, M. Romanowicz, and M. M. Hella, "A gbps building-to-building VLC link using standard CMOS avalanche photodiodes," *IEEE Photon. J.*, vol. 9, no. 6, pp. 1–9, Dec. 2017.

[50] A. T. Hussein, M. T. Alresheedi, and J. M. H. Elmirghani, "Fast and efficient adaptation techniques for visible light communication systems," *J. Opt. Commun. Netw.*, vol. 8, no. 6, pp. 382–397, Jun. 2016.

[51] D. Bykhovsky and S. Arnon, "Multiple access resource allocation in visible light communication systems," *J. Lightw. Technol.*, vol. 32, no. 8, pp. 1594–1600, Apr. 2014.

[52] P. M. Pardalos, A. Žilinskas, and J. Žilinskas, *Non-convex Multi-Objective Optimization*. Springer, 2017.

[53] S. Boyd, S. P. Boyd, and L. Vandenberghe, *Convex Optimization*. Cambridge, U.K.: Cambridge Univ. Press, 2004.

[54] D. E. Goldberg, *Genetic Algorithms*. London, U.K.: Pearson, 2006.

[55] K. Deb, *Multi-Objective Optimization Using Evolutionary Algorithms*, vol. 16. Hoboken, NJ, USA: Wiley, 2001.

[56] X. Yang, Y. Wang, D. Zhang, and L. Cuthbert, "Resource allocation in LTE OFDMA systems using genetic algorithm and semi-smart antennas," in *Proc. IEEE Wireless Commun. Netw. Conf.*, Apr. 2010, pp. 1–6.

[57] N. Sharma and A. S. Madhukumar, "Genetic algorithm aided proportional fair resource allocation in multicast OFDM systems," *IEEE Trans. Broadcast.*, vol. 61, no. 1, pp. 16–29, Mar. 2015.

[58] Z. Wang, C. Yu, W.-D. Zhong, J. Chen, and W. Chen, "Performance of a novel LED lamp arrangement to reduce SNR fluctuation for multi-user visible light communication systems," *Opt. Express*, vol. 20, no. 4, pp. 4564–4573, Jun. 2012.

[59] W. Gu, M. Aminikashani, P. Deng, and M. Kavehrad, "Impact of multipath reflections on the performance of indoor visible light positioning systems," *J. Lightw. Technol.*, vol. 34, no. 10, pp. 2578–2587, May 15, 2016.

[60] R. Zhang, H. Claussen, H. Haas, and L. Hanzo, "Energy efficient visible light communications relying on amorphous cells," *IEEE J. Sel. Areas Commun.*, vol. 34, no. 4, pp. 894–906, Apr. 2016.

[61] K. Lee, H. Park, and J. R. Barry, "Indoor channel characteristics for visible light communications," *IEEE Commun. Lett.*, vol. 15, no. 2, pp. 217–219, Feb. 2011.
[62] A. Nuwanpriya, S.-W. Ho, and C. S. Chen, "Indoor MIMO visible light communications: Novel angle diversity receivers for mobile users," *IEEE J. Sel. Areas Commun.*, vol. 33, no. 9, pp. 1780–1792, Sep. 2015.
[63] Y. S. Eroglu, A. Sahin, I. Guvenc, N. Pala, and M. Yuksel, "Multi-element transmitter design and performance evaluation for visible light communication," in *Proc. IEEE Globecom Workshops (GC Wkshps)*, Dec. 2015, pp. 1–6.

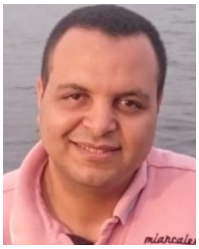

HOSSIEN B. ELDEEB (Member, IEEE) received the B.Sc. degree in electronics and electrical communication engineering from Menoufia University, Menouf, Egypt, in 2008, and the M.Sc. degree in electrical and electronics communication engineering from Cairo University, Cairo, Egypt, in 2017. He is currently pursuing the Ph.D. degree with the Communication Theory and Technologies (CT&T) Research Group, Özyeğin University, Istanbul, Turkey, under the supervision of Prof. M. Uysal. He joined the CT&T Research Group, as a Research Assistant, in 2018. He is also a Research Engineer with the EU-ITN-Vision Project. He has practical experience, as an Instrumentation and Control Engineer with Cairo-West and Giza-North Electrical Power Stations, Giza, Egypt. His current research interests include photonics and optical wireless communications, channel modeling for indoor and outdoor visible light communications, optical system design, raytracing, channel measurements for light communication systems, combining schemes, and diversity techniques. He is a member of the IEEE Society. He received the Best Paper Award from the IEEE/IET CSNDSP in 2020.

MONA HOSNEY was born in Alexandria, Egypt, in 1989. She received the B.S. degree (Hons.) from the Faculty of Engineering, Alexandria University, in 2011. She is currently pursuing the M.S. degree with the Faculty of Engineering, Cairo University. From 2012 to 2013, she was with Huawei. She has been an Instructor in academic and research with the Transmission Department, National Telecommunication Institute, Egypt, since 2013. Her research interests include optical communication, optical fiber, indoor visible light communication, and mobile communication. She received the Certificate on Optical Fiber Installation from Corning.

HANY M. ELSAYED (Member, IEEE) received the B.Sc., M.Sc., and Ph.D. degrees in electronics and communications engineering from Cairo University, in 1980, 1984, and 1988, respectively. He was a Visiting Researcher with LAAS, France, from 1984 to 1987. He held several visiting professor and consultant positions in Egypt and abroad. His research interests include control of networked systems, real-time embedded systems, and wireless sensor networks.

RAGIA I. BADR received the B.Sc. degree (Hons.) from the Electronics and Communications Department, Faculty of Engineering, Cairo University, in 1979, the M.Sc. degree in systems and control Engineering, in 1982, and the Ph.D. degree in systems and control engineering from Cairo University, in 1987. In 1987, she was an Assistant Professor with the Electronics and Communications Department, Faculty of Engineering, Cairo University, where she is currently a Professor. Her research interests include robust control, neuro-fuzzy control, and adaptive-non-linear control.

MURAT UYSAL (Fellow, IEEE) received the B.Sc. and M.Sc. degrees in electronics and communication engineering from Istanbul Technical University, Istanbul, Turkey, in 1995 and 1998, respectively, and the Ph.D. degree in electrical engineering from Texas A&M University, College Station, TX, USA, in 2001.

He was a tenured Associate Professor with the University of Waterloo, Canada. He is currently a Full Professor and the Chair of the Department of Electrical and Electronics Engineering, Özyeğin University, Istanbul. He is also the Founding Director with the Center of Excellence in Optical Wireless Communication Technologies (OKATEM). He has authored over 350 journal and conference papers on these topics and received more than 13,000 citations with a h-index of 56. He was involved in the organization of several the IEEE conferences at various levels. His research interests include communication theory with a particular emphasis on physical layer aspects of wireless communication systems in radio and optical frequency bands.

Dr. Uysal served as the Technical Program Committee Chair for the major IEEE conferences, including WCNC in 2014, PIMRC in 2019, and VTC-Fall in 2019. He serves as the former Chair for the IEEE Turkey Section. He received major distinctions, include the NSERC Discovery Accelerator Award in 2008, the University of Waterloo Engineering Research Excellence Award in 2010, the Turkish Academy of Sciences Distinguished Young Scientist Award in 2011, the Ozyegin University Best Researcher Award in 2014, the National Instruments Engineering Impact Award in 2017, the Elginkan Foundation Technology Award in 2018, the IEEE Communications Society Best Survey Paper Award in 2019, and so on. He served as an Editor for the IEEE TRANSACTIONS ON COMMUNICATIONS, the IEEE TRANSACTIONS ON VEHICULAR TECHNOLOGY, and the IEEE COMMUNICATIONS LETTERS. He serves on the Editorial Board of the IEEE TRANSACTIONS ON WIRELESS COMMUNICATIONS.

HOSSAM A. I. SELMY (Member, IEEE) was born in Giza, Egypt, in 1979. He received the B.S. and M.S. degrees in electrical engineering from Cairo University, Cairo, Egypt, in 2001 and 2007, respectively, and the Ph.D. degree in electrical engineering from the Egypt Japan University of Science and Technology, Alexandria, Egypt, in 2013. He is currently an Associate Professor with the National Institute of Laser Enhanced Science (NILES), Cairo University. His publication topics, include free-space optical communication, optimization, resource allocation, 5G mobile communication, optical links, radio access networks, OFDM modulation, cloud computing, error statistics, optical transceivers, telecommunication network reliability, 4G mobile communication, long term evolution, channel capacity, continuous phase modulation, discrete Fourier transforms, millimetre-wave communication, mobile radio, optical modulation, precoding, quadrature amplitude modulation, radio links, radio-over-fiber, radiofrequency interference, and optical fiber communication. His research interests include advanced modulation and multiple access schemes for optical fiber communication and next-generation wireless access networks.